

Coupled spin and pseudomagnetic field in graphene nanoribbons

Wen-Yu He and Lin He*

Department of Physics, Beijing Normal University, Beijing, 100875, People's Republic of China

(Received 1 May 2013; published 9 August 2013)

A pseudomagnetic field becomes an experimental reality after the observation of zero-field Landau level-like quantization in strained graphene, but it is not expected that the time-reversal symmetric pseudomagnetic fields will have any effect on the spin degree of freedom of the charge carriers. Here, we demonstrate that spin-orbit coupling (SOC) could act as a bridge between the pseudomagnetic field and spin. In quantum spin Hall (QSH) states, the direction of the spin of edge states is tied to their direction of motion because of the SOC. The pseudomagnetic field affects the clockwise and counterclockwise edge currents of the QSH states and consequently lifts the degenerate edge states of opposite spin orientation. Because of opposite signs of the pseudomagnetic field in two valleys of graphene, the one-dimensional charge carriers at the two opposite edges have different group velocities, and in some special cases, the edge states can only propagate at one edge of the nanoribbon, and the group velocity at the other edge becomes zero.

DOI: [10.1103/PhysRevB.88.085411](https://doi.org/10.1103/PhysRevB.88.085411)

PACS number(s): 72.80.Vp, 73.20.-r, 73.43.-f, 73.61.Wp

I. INTRODUCTION

Generally speaking, we divide the effects of a real magnetic field on charge carriers into two parts: the orbital field and the Zeeman field. The orbital field influences the electronic motion by introducing unimodular phase factors in the electron hopping amplitudes, and the Zeeman field lifts the energy degenerate states of opposite spin orientation. In graphene, a strain-induced hopping modulation between sublattices affects the Dirac fermions like an effective gauge field (pseudomagnetic field) and can result in partially flat bands in the band structure of graphene at discrete energies, which are the analog of Landau levels in real magnetic fields.¹⁻³ Such pseudomagnetic fields become an experimental reality after the observation of zero-field Landau level-like quantization in strained graphene.⁴⁻⁹ The slight difference between the pseudomagnetic field and the orbital magnetic field is that the pseudomagnetic field preserves time-reversal symmetry and has opposite signs for charge carriers in the two low-energy valleys, K and K' . Because it lacks the Zeeman term, therefore, the pseudomagnetic field is not expected to have any effect on the spin degree of freedom of the charge carriers.^{2,3}

Here, we present theoretical investigations of the pseudomagnetic fields in strained graphene, and we show that the pseudomagnetic fields can affect the spin degree of freedom through spin-orbit coupling, which links spin and momentum of the charge carriers. Our results indicate that the pseudomagnetic fields can lift the degenerate edge states of opposite spin orientation in zigzag graphene nanoribbons and produce asymmetry of the quantum spin Hall (QSH) states: the spin-polarized edge states have different group velocities at the two opposite edges, and in some special cases, the edge states propagate without dissipation at one edge of the nanoribbon, and the group velocity at the opposite edge becomes zero. Our result opens a new door to explore spin-based electronics in graphene.

II. HAMILTONIAN OF GRAPHENE NANORIBBON

The proposal of the QSH states (or the topological edge states) in graphene was a milestone in the development of

the field of topological insulator.¹⁰⁻¹⁵ However, graphene's extremely weak intrinsic spin-orbit coupling makes the realization of the QSH states practically unrealistic.^{16,17} Recently, recipes for enhancing spin-orbit interaction on graphene by the introduction of adatoms have been suggested.¹⁸⁻²¹ Experimentally, it was demonstrated that small amounts of covalently bonded hydrogen atoms induce a colossal enhancement of the spin-orbit coupling in graphene by three orders of magnitude, i.e., the spin-orbit coupling increases from the order of 10^{-3} meV to ~ 2.5 meV.²² Thus, the experimental study of graphene with a moderate strength of spin-orbit interaction now appears feasible, and it becomes possible to realize the QSH states in graphene at an experimentally accessible temperature.

In the tight-binding model of graphene with the spin-orbit interaction, the Hamiltonian takes the form,^{10,11}

$$H = \sum_{\langle ij \rangle \alpha} t c_{i\alpha}^\dagger c_{j\alpha} + \sum_{\langle\langle ij \rangle\rangle \alpha\beta} i t_2 v_{ij} s_{\alpha\beta}^z c_{i\alpha}^\dagger c_{j\beta}. \quad (1)$$

Here, the first term is the nearest-neighbor hopping term on the honeycomb lattice, t is the hopping integral, and the operators $c_{i\alpha}^\dagger$ ($c_{i\alpha}$) create (annihilate) an electron with spin α at site i . Around the Dirac points, the first term becomes a two-dimensional massless Dirac equation, which describes the low-energy behaviors of the charge carriers in the graphene monolayer.¹ The second term of the Hamiltonian (1) describes the spin-orbit interaction by introducing a spin-dependent second-neighbor hopping t_2 . Here, $v_{ij} = \pm 1$, depending on the orientation of the two nearest-neighbor bonds the electron traverses in going from site j to i , and $s_{\alpha\beta}^z$ is the Pauli matrix describing the electron's spin.^{10,11} The QSH states can be obtained by solving Hamiltonian (1) in a nanoribbon geometry, as shown in Fig. 1. In the QSH states, the electrons with opposite spin orientation propagate in the opposite directions at each edge, and the electrons with the same spin orientation between the two opposite edges also propagate in opposite directions.^{10,11} For a zigzag graphene nanoribbon, the QSH states become a nontopological surface states when the spin-orbit coupling is vanishingly small.^{10,23}

When only the first term of the Hamiltonian (1) is taken into account, the strain-induced lattice deformations change

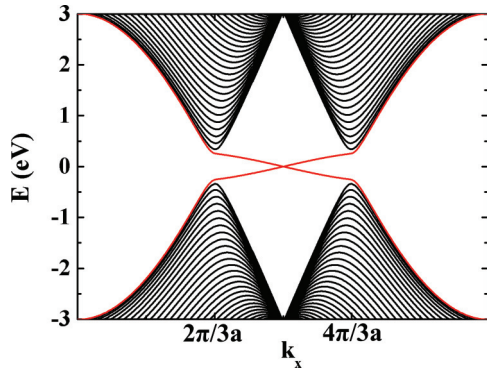


FIG. 1. (Color online) One-dimensional band structure of a zigzag graphene nanoribbon with $N = 60$ and $t_2/t = 0.05$. The bands crossing the gap are spin-filtered edge states.

the electron hopping between sublattices and give rise to an effective gauge field \mathbf{A} in the Dirac equation. Certain spatially varying deformation patterns affect the Dirac fermions in graphene, mimicking the effect of uniform pseudomagnetic fields $B_S = \nabla \times \mathbf{A}$. Figure 2 shows a concrete lattice to realize a uniform pseudomagnetic field with $A_x = \frac{c}{ev_F} (t - t_1) = B_S y$

and $A_y = 0$. The pseudomagnetic field cannot lift the degenerate band of opposite spin orientation, and we obtain a twofold degenerate band structure even when the spin degree of freedom is considered. For the zigzag graphene nanoribbon, the pseudomagnetic fields have opposite signs in the two valleys (K and K'), which play a vital role in the emergence of the asymmetric QSH states.

III. EFFECT OF PSEUDOMAGNETIC FIELDS AND SPIN-ORBIT COUPLING

When both the pseudomagnetic fields and the spin-orbit coupling are taken into account, the pseudomagnetic fields lift the degenerate edge states of opposite spin orientation through the spin-orbit coupling, which links the spin and momentum of the charge carriers. Consequently, we obtain a new and unique QSH state in zigzag graphene nanoribbons. Figure 3 shows the one-dimensional energy bands for a zigzag graphene nanoribbon. The electronic states of opposite spin orientation are still degenerate in all “bulk” bands, and the valley-dependent pseudomagnetic fields only lift the degenerate edge states. The energy-level shifts are of opposite signs for the degenerate edge states in the two valleys.

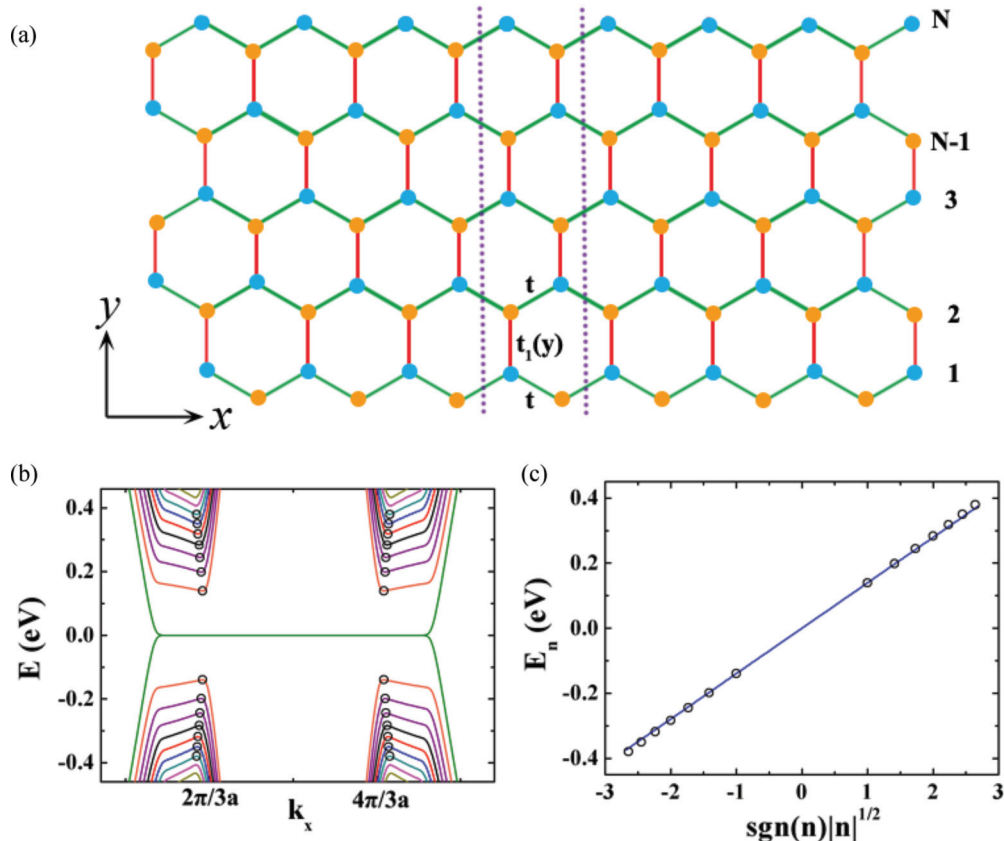


FIG. 2. (Color online) A zigzag graphene nanoribbon in uniform pseudomagnetic fields. (a) Diagram of a zigzag graphene nanoribbon. The hopping matrix element along the y direction (red bonds) is changed to induce the gauge field $A_x = B_S y$ and $A_y = 0$. N is the number of zigzag chains in the nanoribbon. (b) Energy dispersion for the graphene nanoribbon in (a). The strain-induced Landau-level-like flat bands acquire a small linear dispersion because of the hybridization with the nontopological surface states of the zigzag nanoribbon. (c) A comparison between energies of the black open circles in (b) and the Landau levels generated in real magnetic fields. The blue line is calculated according to $E_n = \text{sgn}(n) \hbar \omega_c \sqrt{|n|}$, where n is the index of the Landau levels and $\omega_c = \sqrt{2e\hbar v_F^2 B_S}$ with v_F as the Fermi velocity and the pseudomagnetic fields $|B_S| = 15.2$ T.

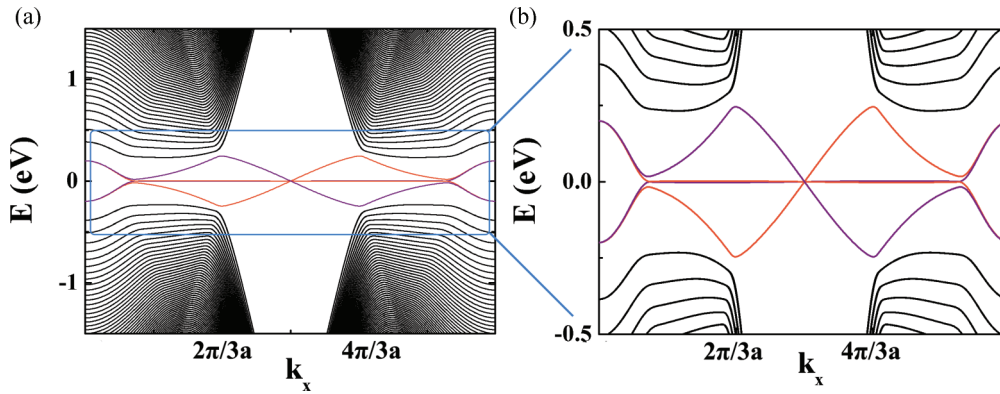


FIG. 3. (Color online) One-dimensional energy dispersion for a zigzag graphene nanoribbon with $N = 600$. (a) and (b) Both the uniform pseudomagnetic fields $|B_S| = 25.90$ T and the spin-orbit coupling ($t_2/t = 0.05$) are taken into account in the calculation. Here, $B_S = 25.90$ T in the K valley and $B_S = -25.90$ T in the K' valley (we define direction of the pseudomagnetic field “down” as positive; “up” as the negative pseudomagnetic field). The orange color denotes the spin-down edge states; violet denotes the spin-up edge states. (b) The low-energy band in (a) is shown. Because of opposite signs of the pseudomagnetic fields in the two valleys, the pseudomagnetic fields induce energy-level shifts of opposite signs for the degenerate edge states of opposite spin orientation. One spin-up edge state and one spin-down edge state become perfectly flat.

For the pseudomagnetic fields used in the calculation, the energies of edge states with spin up (spin down) are raised (lowered) for the states with $k_x < \pi/a$ (here, π/a is the Brillouin zone boundary), i.e., in the K valley. The energies of edge states with spin up (spin down) are lowered (raised) for the states with $k_x > \pi/a$, i.e., in the K' valley. If we switch the direction of the pseudomagnetic fields in the K valley, then the energies of edge states with spin up (spin down) are lowered

(raised) for the states with $k_x < \pi/a$. The crossing of the states at the Brillouin zone boundary $k_x = \pi/a$ is protected by time-reversal symmetry.^{10,11} Therefore, the degeneracy of the edge states at $k_x = \pi/a$ cannot be lifted by the pseudomagnetic field.

To understand the physics behind this phenomenon, we have carried out the same calculation in a static orbital magnetic field (the Zeeman field is not included in the

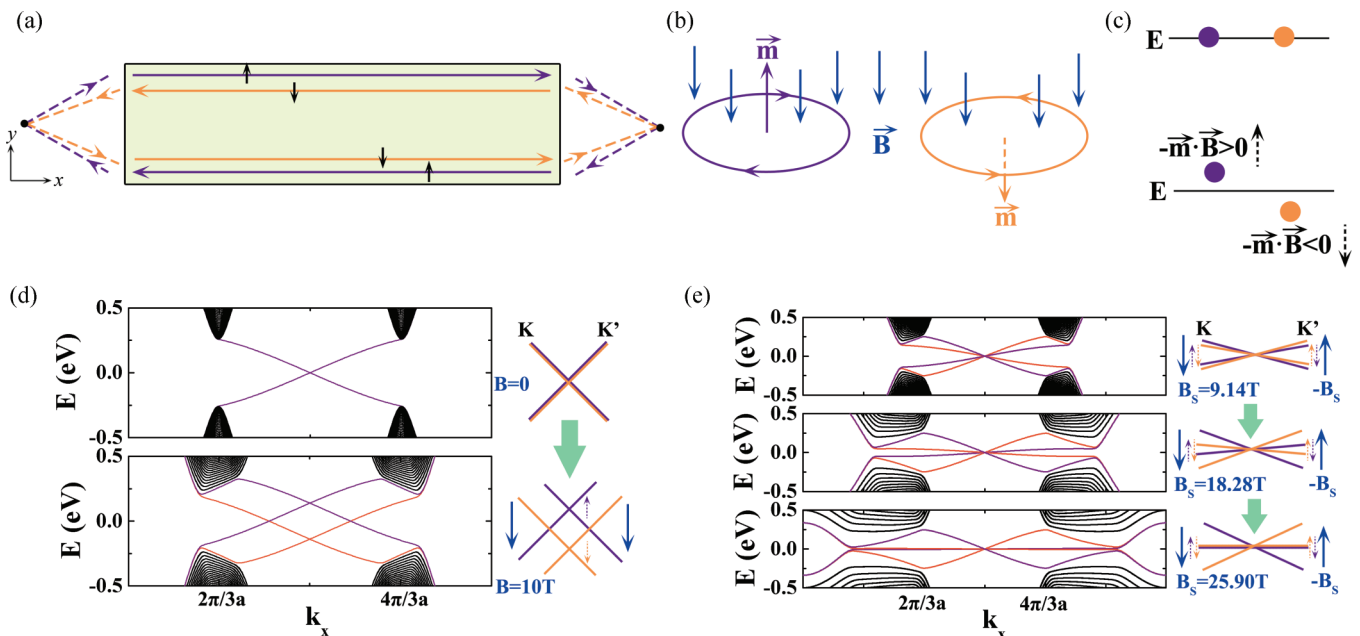


FIG. 4. (Color online) Origin of the asymmetric QSH states in graphene nanoribbons. (a) Schematic diagram showing the QSH states in a graphene nanoribbon. The spin-up and spin-down electrons propagate clockwise and counterclockwise, respectively. (b) and (c) The interplay between the orbital magnetic field (or the pseudomagnetic field) and effective magnetic moments generated by the clockwise and counterclockwise edge currents lifts the degeneracy of the edge states. (d) Upper panel: energy dispersion of a zigzag graphene nanoribbon with $N = 600$ in a zero magnetic field. Lower panel: energy dispersion of the zigzag graphene nanoribbon in a static orbital magnetic field $B = 10$ T. In both valleys, the energy of the clockwise edge states (spin-up electrons) is raised, and the energy of the counterclockwise edge states (spin down electrons) is lowered. (e) The low-energy bands of the zigzag graphene nanoribbon in different values of the pseudomagnetic fields.

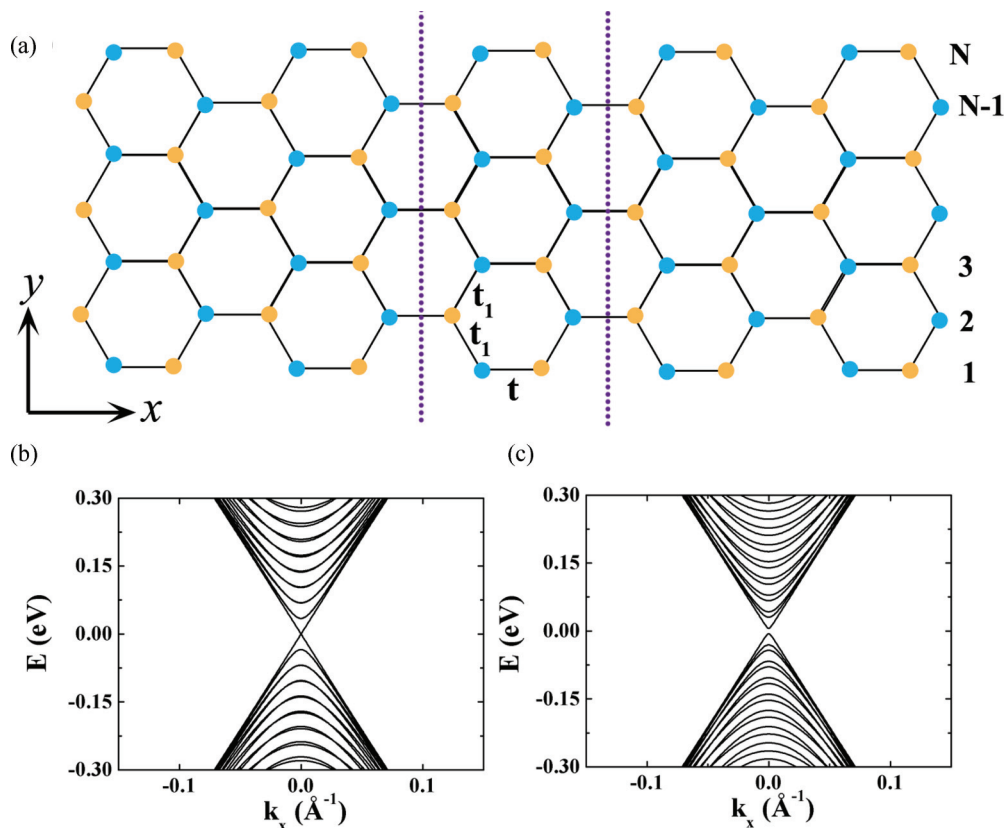


FIG. 5. (Color online) (a) Diagram of an armchair graphene nanoribbon. (b) The energy spectrum of the armchair graphene nanoribbon considering the spin-orbit coupling. (c) The energy spectrum of the armchair graphene nanoribbon considering both the pseudomagnetic field and the spin-orbit coupling.

calculation, and the direction of the magnetic field is the same in the two valleys). With introducing the orbital magnetic field, the hopping integral t_{ij} is replaced by $t_{ij}e^{i2\pi\varphi_{i,j}}$, where $\varphi_{i,j}$ is given by the line integral of the vector potential from site i to j . In both valleys, the energy of the clockwise edge states (spin-up electrons) is raised, and the energy of the counterclockwise edge states (spin-down electrons) is lowered by the orbital magnetic field, as shown in Fig. 4. This result indicates that the spin-split edge states are induced by the interplay between the orbital magnetic field (or the pseudomagnetic field) and the clockwise and counterclockwise edge currents (Fig. 4). The spin-orbit coupling links the spin and the momentum, the spin of an electron that has been affected is determined by its momentum (whether the edge currents is clockwise or counterclockwise). Therefore, the spin-orbit coupling acts as a bridge between the pseudomagnetic field and the spin degree of freedom. For armchair graphene nanoribbons, the effect of pseudomagnetic fields on the edge states is perfectly canceled in the K and K' valleys, as shown in Fig. 5. Therefore, the asymmetric QSH effect can only be observed in zigzag graphene nanoribbons.

The opposite signs of pseudomagnetic fields in the K and K' valleys of zigzag graphene nanoribbons lead to opposite signs of energy-level shifts for the degenerate edge states in the two valleys, as shown in Fig. 4. This is the key factor for the emergence of the asymmetric QSH states. The pseudomagnetic fields lead to asymmetric group velocities of the edge states at opposite edges of the nanoribbon. In some peculiar values of the pseudomagnetic fields, both the spin-up

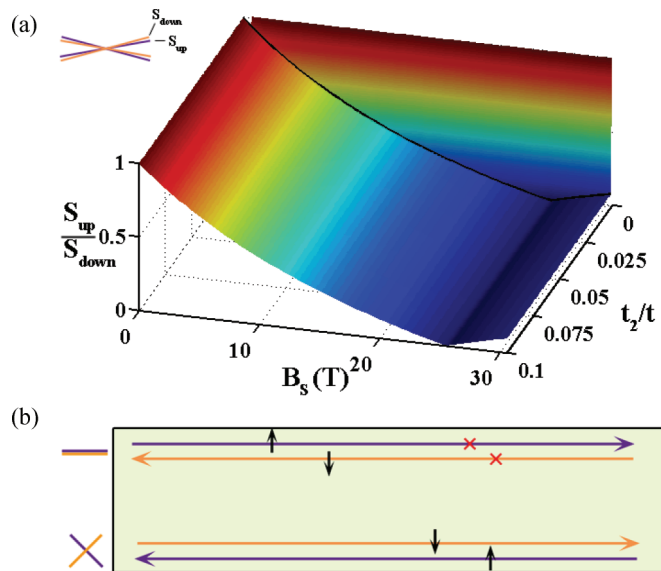


FIG. 6. (Color online) The asymmetric QSH states in a graphene nanoribbon. (a) The ratio of S_{up}/S_{down} as a function of the pseudomagnetic fields and the strength of spin-orbit coupling. S_{up} and S_{down} are the slope of edge states in the K' valley with spin-up and spin-down, respectively. The solid black line is plotted to show the ratio of S_{up}/S_{down} as a function of the pseudomagnetic fields for $t_2/t = 0.001$. The system becomes asymmetric QSH state when $S_{up}/S_{down} = 0$. (b) Schematic diagram showing the asymmetric QSH states in a graphene nanoribbon. The group velocity of the QSH states becomes zero at one edge of the nanoribbon.

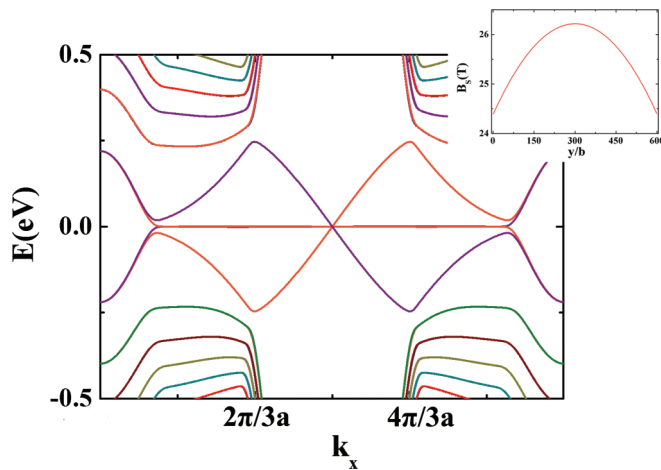


FIG. 7. (Color online) The energy spectrum of a zigzag graphene nanoribbon in nonuniform pseudomagnetic fields. The inset shows the distribution of pseudomagnetic field along the y direction, where $b = \frac{\sqrt{3}}{2}a$. The asymmetric QSH states still can be obtained.

and spin-down edge states at one edge of the nanoribbon become perfectly flat, as shown in Figs. 3 and 4. Then, the group velocity of the edge states becomes zero. It indicates that the QSH states only propagate in a dissipationless way at one edge of the nanoribbon, and the edge state is suppressed at the opposite edge, as shown in Fig. 6. In QSH states, the edge states are not chiral because each edge has electrons that propagate in both directions and the counterpropagation of the same spin states at the two opposite edges. When the group velocity at one edge of the nanoribbon becomes zero, the graphene nanoribbon provides dissipationless spin-polarized current only at one edge, and the edge states become chiral. Then, the graphene nanoribbon acts as a dissipationless “spin battery,”²⁴ and the edge states could be used as a dissipationless spin-filtering path for spintronic devices. The asymmetric QSH state is distinct from other existing quantum Hall-related effects (i.e., the quantum Hall effect, the QSH effect, and the quantum anomalous Hall effect) and adds a new member in the quantum Hall family.²⁵

The asymmetric QSH states can exist, and the asymmetry is obvious for $t_2/t = 0.001$, as shown in Fig. 6. It indicates that our theoretical results hold well for the strength of spin-orbit interaction in the range accessible by experiments.²¹ By taking advantage of the development in the fabrication of graphene nanoribbons,²⁶ we believe that the experimental detection of the asymmetric QSH state is possible. The

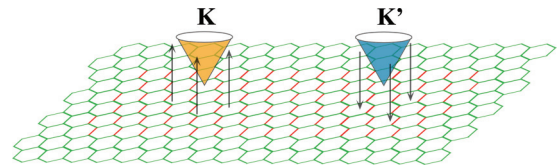


FIG. 8. (Color online) Schematic diagram showing a zigzag graphene nanoribbon in nonuniform pseudomagnetic fields. The asymmetric QSH states could be observed in the graphene nanoribbons with a part of the deformed structure.

asymmetric QSH states could be observable by studying low-temperature charge transport^{13,27} in weakly hydrogenated zigzag graphene nanoribbons with a deformed structure. Other graphene sheet analogs with strong spin-orbit coupling^{28,29} and lattice deformations should also exhibit this effect.

In the preceding calculation, we used a uniform pseudomagnetic field to induce the asymmetric QSH states in graphene nanoribbons. Actually, this is not necessary for the emergence of the asymmetric QSH states. The asymmetric QSH states also exist in zigzag graphene nanoribbons with nonuniform pseudomagnetic fields, as shown in Fig. 7, and it could be observed in graphene nanoribbons with a small part of a deformed structure, as shown in Fig. 8. The asymmetry of the edge states at opposite edges of the nanoribbon is robust when the net pseudomagnetic field of the nanoribbon is not zero in a valley.

IV. CONCLUSION

In summary, we show that the time-reversal symmetric pseudomagnetic fields can affect the spin of charge carriers through spin-orbit coupling, and the pseudomagnetic fields lift the degenerate edge states of opposite spin orientation in zigzag graphene nanoribbons. This effect not only results in asymmetric QSH states in graphene nanoribbons but also opens a new door to explore spin-based electronics in graphene.

ACKNOWLEDGMENTS

The authors would like to thank Hua Jiang, Cheng-cheng Liu, and Yugui Yao for helpful discussions. We are grateful to the National Key Basic Research Program of China (Grants No. 2013CBA01603 and No. 2014CB920903) and the National Science Foundation (Grant No. 11004010), and the Fundamental Research Funds for the Central Universities.

*Corresponding author: helin@bnu.edu.cn

¹A. H. Castro Neto, F. Guinea, N. M. R. Peres, K. S. Novoselov, and A. K. Geim, *Rev. Mod. Phys.* **81**, 109 (2009).

²M. A. H. Vozmediano, M. I. Katsnelson, and F. Guinea, *Phys. Rep.* **496**, 109 (2010).

³M. I. Katsnelson, K. S. Novoselov, and A. K. Geim, *Nat. Phys.* **2**, 620 (2006).

⁴N. Levy, S. A. Burke, K. L. Meaker, M. Panlasigui, A. Zettl, F. Guinea, A. H. Castro Neto, and M. F. Crommie, *Science* **329**, 544 (2010).

⁵H. Yan, Y. Sun, L. He, J. C. Nie, and M. H. W. Chan, *Phys. Rev. B* **85**, 035422 (2012).

⁶K. K. Gomes, W. Mar, W. Ko, F. Guinea, and H. C. Manoharan, *Nature (London)* **483**, 306 (2012).

- ⁷D. Guo, T. Kondo, T. Machida, K. Iwatake, S. Okada, and J. Nakamura, *Nat. Commun.* **3**, 1068 (2012).
- ⁸L. Meng, W.-Y. He, H. Zheng, M. Liu, H. Yan, W. Yan, Z.-D. Chu, K. Bai, R.-F. Dou, Y. Zhang, Z. Liu, J.-C. Nie, and L. He, *Phys. Rev. B* **87**, 205405 (2013).
- ⁹W. Yan, W.-Y. He, Z.-D. Chu, M. Liu, L. Meng, R.-F. Dou, Y. Zhang, Z. Liu, J.-C. Nie, and L. He, *Nat. Commun.* **4**, 2159 (2013).
- ¹⁰C. L. Kane and E. J. Mele, *Phys. Rev. Lett.* **95**, 226801 (2005).
- ¹¹C. L. Kane and E. J. Mele, *Phys. Rev. Lett.* **95**, 146802 (2005).
- ¹²B. A. Bernevig, T. L. Hughes, and S.-C. Zhang, *Science* **314**, 1757 (2006).
- ¹³M. Konig, S. Wiedmann, C. Brune, A. Roth, H. Buhmann, L. W. Molenkamp, X.-L. Qi, and S.-C. Zhang, *Science* **318**, 766 (2007).
- ¹⁴M. Z. Hasan and C. L. Kane, *Rev. Mod. Phys.* **82**, 3045 (2010).
- ¹⁵X.-L. Qi and S.-C. Zhang, *Rev. Mod. Phys.* **83**, 1057 (2011).
- ¹⁶H. Min, J. E. Hill, N. A. Sinitsyn, B. R. Sahu, L. Kleinman, and A. H. MacDonald, *Phys. Rev. B* **74**, 165310 (2006).
- ¹⁷Y. Yao, F. Ye, X.-L. Qi, S.-C. Zhang, and Z. Fang, *Phys. Rev. B* **75**, 041401 (2007).
- ¹⁸H. Jiang, Z. Qiao, H. Liu, J. Shi, and Q. Niu, *Phys. Rev. Lett.* **109**, 116803 (2012).
- ¹⁹C. Weeks, J. Hu, J. Alicea, M. Franz, and R. Wu, *Phys. Rev. X* **1**, 021001 (2011).
- ²⁰J. Hu, J. Alicea, R. Wu, and M. Franz, *Phys. Rev. Lett.* **109**, 266801 (2012).
- ²¹O. Shevtsov, P. Carmier, C. Groth, X. Waintal, and D. Carpentier, *Phys. Rev. B* **85**, 245441 (2012).
- ²²J. Balakrishnan, G. K. W. Koon, M. Jaiswal, A. H. Castro Neto, and B. Ozyilmaz, *Nat. Phys.* **9**, 284 (2013).
- ²³Y.-W. Son, M. L. Cohen, and S. G. Louie, *Nature (London)* **444**, 347 (2006).
- ²⁴A. Brataas, Y. Tserkovnyak, G. E. W. Bauer, and B. I. Halperin, *Phys. Rev. B* **66**, 060404 (2002).
- ²⁵S. Oh, *Science* **340**, 153 (2013).
- ²⁶J. Cai, P. Ruffieux, R. Jaafar, M. Bieri, T. Braun, S. Blankenburg, M. Muoth, A. P. Seitsonen, M. Saleh, X. Feng, K. Mullen, and R. Fasel, *Nature (London)* **466**, 470 (2010).
- ²⁷C.-Z. Chang, J. Zhang, X. Feng, J. Shen, Z. Zhang, M. Guo, K. Li, Y. Ou, P. Wei, L.-L. Wang, Z.-Q. Ji, Y. Feng, S. Ji, X. Chen, J. Jia, X. Dai, Z. Fang, S.-C. Zhang, K. He, Y. Wang, L. Lu, X.-C. Ma, and Q.-K. Xue, *Science* **340**, 167 (2013).
- ²⁸C.-C. Liu, W. Feng, and Y. Yao, *Phys. Rev. Lett.* **107**, 076802 (2011).
- ²⁹B. Rasche, A. Isaeva, M. Ruck, S. Borisenko, V. Zabolotnyy, B. Buchner, K. Koepf, C. Ortix, M. Richter, and J. van den Brink, *Nat. Mater.* **12**, 422 (2013).